

nffa.eu

PILOT 2021 2026

DELIVERABLE REPORT

WP11 JA1 - Real-time observation and control in microscopy and spectroscopy of nano-objects

D11.5

Determination of the DMI constant by fourwave mixing FWM experiments based on a table top laser

Due date

M18



This initiative has received funding from the EU's H2020 framework program for research and innovation under grant agreement n. 101007417, NFFA-Europe Pilot Project

PROJECT DETAILS

PROJECT ACRONYM

NEP

PROJECT TITLE

Nanoscience Foundries and Fine Analysis - Europe|PILOT

GRANT AGREEMENT NO:

101007417

FUNDING SCHEME

RIA - Research and Innovation action

START DATE

01/03/2021

WORK PACKAGE DETAILS

WORK PACKAGE ID

WP 11

WORK PACKAGE TITLE

Real-time observation and control in microscopy and spectroscopy of nano-objects

WORK PACKAGE LEADER

Prof. Giovanni De Ninno (UNG)

DELIVERABLE DETAILS

DELIVERABLE ID

D11.5

DELIVERABLE TITLE

Determination of the DMI constant by four-wave mixing FWM experiments based on a table top laser.

DELIVERABLE DESCRIPTION

Implementation of a new experimental setup for measuring the magnetic properties based on transient grating approach

DUE DATE

18 (Month) 31/08/2022

ACTUAL SUBMISSION DATE

31/08/2022

AUTHORS

Riccardo Cucini (CNR)



PERSON RESPONSIBLE FOR THE DELIVERABLE

Riccardo Cucini (CNR)

NATURE

- R - Report
- P - Prototype
- DEC - Websites, Patent filing, Press & media actions, Videos, etc
- O - Other

DISSEMINATION LEVEL

- P - Public
- PP - Restricted to other programme participants & EC: (Specify)
- RE - Restricted to a group (Specify)
- CO - Confidential, only for members of the consortium



REPORT DETAILS

ACTUAL SUBMISSION DATE	NUMBER OF PAGES
31/08/2022	12

FOR MORE INFO PLEASE CONTACT

Riccardo Cucini
CNR - IOM
Strada Statale 14 - km 163,5 in
AREA Science Park
34149 Basovizza, Trieste ITALY

email: cucini@iom.cnr.it

VERSION	DATE	AUTHOR(S)	DESCRIPTION / REASON FOR MODIFICATION	STATUS
1	09/08/2022			Draft
2	22/08/2022			Final
				Choose an item.
				Choose an item.
				Choose an item.
				Choose an item.

CONTENTS

Introduction	5
Experimental progress	6
Pulsed TG setup	6
Faraday probe setup	8
Results and discussion	9



INTRODUCTION

During the first year of NEP project a new setup for Four-Wave-Mixing (FWM) experiment was under development and implementation. Due to some problems with the laser amplifier and oscillator, the experiment was stopped for almost one year. Knowing the long time generally required for repairing this systems, we decide to implement the setup using a different type of laser, which furnishes pulses with 300 fs time length, a repetition rate of 100 kHz, and 400 uJ/pulse at 1030 nm. The main scope of this deliverable is demonstrating if it is possible to measure magnetic properties with a FWM approach, and comparing it with well-known technique for magnetic measurements.

The chosen approach is the Transient Grating (TG), which is one of the possible technique in the framework of FWM approach. The system was installed to the SPRINT lab of the Istituto Officina dei Materiali (IOM) of Consiglio Nazionale delle Ricerche (CNR) in Trieste.

In a TG experiment a single pulsed laser beam is split to obtain two laser pulses, which interfere within the sample to generate the so-called TG, a spatially periodic variation of the optical material properties by standing-wave excitation of some material modes. The spatial modulation of the material optical properties acts as a diffraction grating lasting the time of overlapping pulses. Its spatial extension is given by the pulses temporal length and its efficiency depends on the overlap area of the two pump pulses. This modulation is probed by a third laser beam of different wavelength, which can be a pulsed or a continuous-wave field. It impinges on the TG-induced modulation and it is diffracted by it. A measurement of the intensity of the diffracted beam at selected time delays with respect to the pump allows the acquisition of dynamic information on the relaxing TG, and consequently of the properties of the excited modes.

The implemented setup was able to optically generate surface acoustic waves (SAW), also seeding coherent spin waves via magneto elastic coupling in ferromagnetic media. In details, we report on SAW-driven ferromagnetic resonance (FMR) experiments performed on polycrystalline Ni thin films in combination with time-resolved Faraday polarimetry, which allows to extract the value of the effective magnetization and of the Gilbert damping. The results are in full agreement with measurements on the very same samples from standard FMR.

The proposed setup demonstrates the possibility to measure magnetic properties in thin films. This opens the way for studying very special magnet interaction, like Dzyaloshinskii-Moriya Interaction (DMI), which is a crucial ingredient for stabilizing chiral spin textures, such as chiral domain walls and skyrmions.



EXPERIMENTAL PROGRESS

Pulsed TG setup

The source is a Yb:KGW-based integrated femtosecond laser system (PHAROS, LightConversion), characterized by a turn-key operation and by high pulse-to-pulse stability. The system produces 300 fs pulses at 1030 nm with a tunable repetition rate from single-shot to 1 MHz. The repetition rate used for the experiment is fixed at 100 kHz.

This section describes the optical setup we built to perform TG measurements in both reflection and transmission geometry. A picture of the optical table is shown in Figure 1, while Figure 2 depicts a sketch of the TG experimental setup.

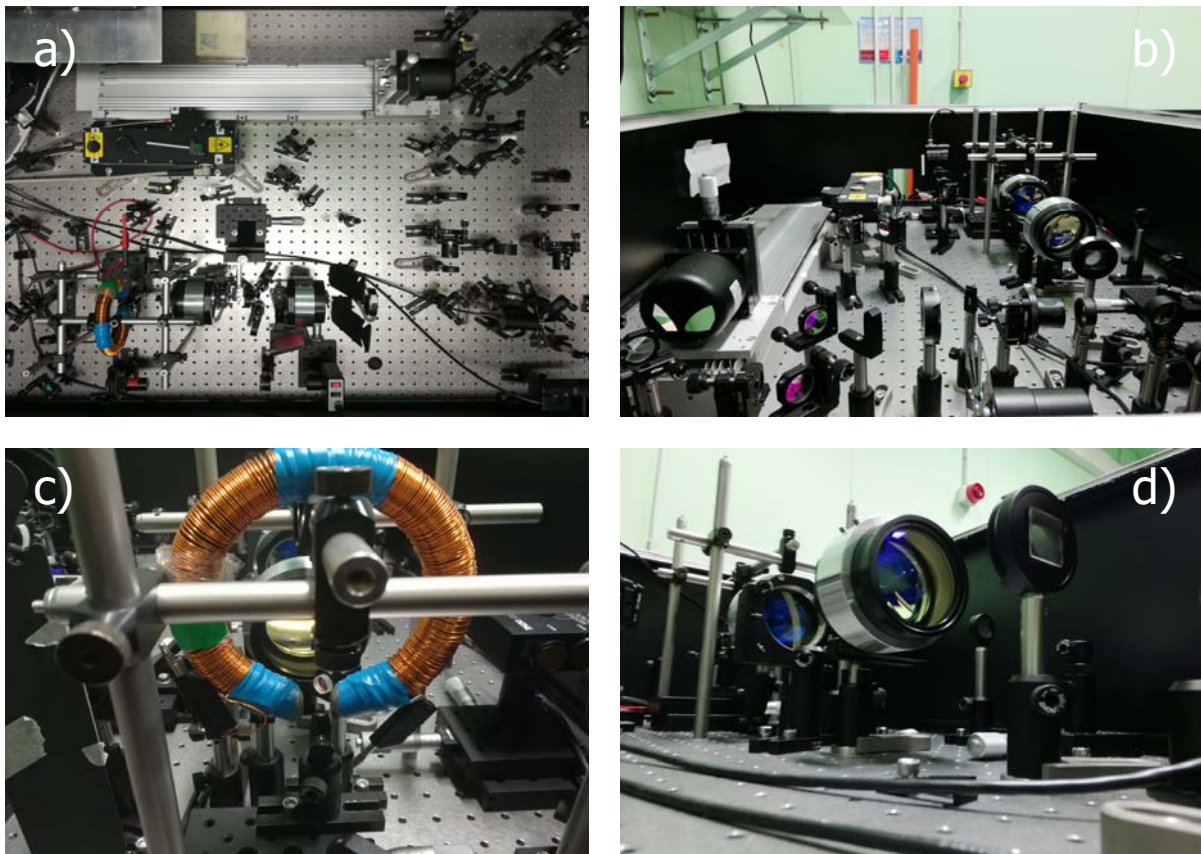


Figure 1: Transient Grating setup; (a) top view (laser not shown), (b) side view, (c) Electromagnet and sample zone. Up to 1000 G magnetic field available. (d) Details of special large doublets and home-made phase mask.

Infrared pump pulses at 1030 nm wavelength and with temporal length of 300 fs are produced the regenerative amplifier of the PHAROS laser source. As the average power is 20 W, 10% of its output

is enough to run our experiment. This allows to work in a parasitic way when the PHAROS is simultaneously used as laser source in some other experiments.

The beam is then split again by a 70/30 beamsplitter: 70% is used for the pump while the remaining 30% passes through a Beta-Barium Borate (BBO) crystal properly oriented to get the phase matching condition and to obtain Second Harmonic Generation (SHG). The harmonics are then divided by a harmonic separator, which reflects only the second harmonic (515 nm).

In order to finely tune the fluence on sample, a $\lambda/2$ waveplate followed by a polarizer is placed along both the pump (WP1, P1) and probe (WP2, P2) branches. Pump and probe are collinearly coupled by the harmonic separator and focused on a phase mask by plano-convex lenses (L1, L2) with focal length $f = 20$ cm. Upon diffraction by the phase mask, the diffraction maxima are recombined by the doublets (D1, D2) in a confocal configuration. The first diffraction orders of the 1030 nm are

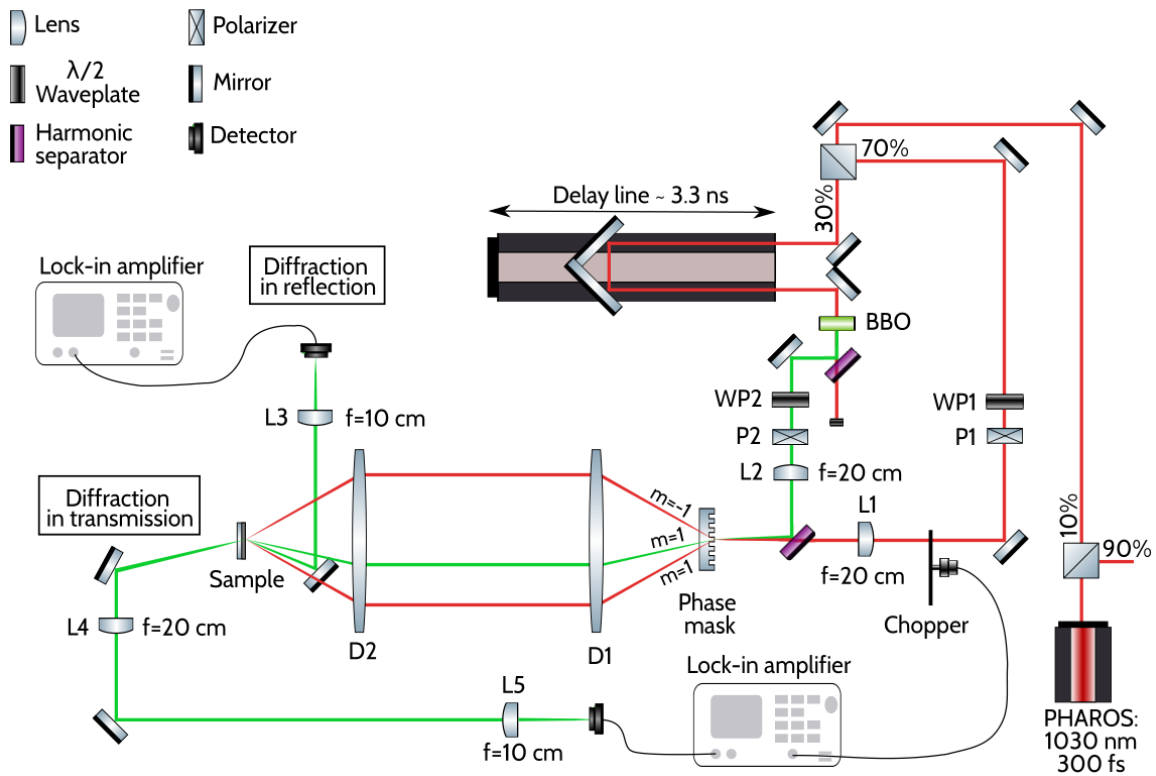


Figure 2: Pulsed TG setup scheme in reflection and transmission geometry. The laser source is the PHAROS, which generates 300 fs pulses at 1030 nm. Just 10% of its output is actually used. A second beamsplitter splits the beam again and the 30% of it passes through the delay line and across the BBO crystal. The harmonic separator provides a pulsed probe with a wavelength of 515 nm. Attenuation of the two beam is possible thanks to the waveplates (WP1, WP2) and the polarizers (P1, P2) placed on each branch. Both pump and probe are then focused with plano-convex lenses (L1, L2) on the phase mask and diffracted. Two identical doublets (D1, D2) in confocal configuration recombine them. One of the first orders of the 515 nm is used as the probe. The pump consists in the two first diffraction orders of the 1030 nm. All other diffraction orders are stopped by a beam blocker.

used as the pump, while the probe consists in one of the first diffraction orders of the 515 nm. All other diffraction orders are stopped by a beam blocker.

The scattered beam is collimated by L4 ($f = 20$ cm) and focalized in a 2151 Newport femtowatt photoreceiver by L5 ($f = 10$ cm). This photoreceiver is an extremely sensitive detector to be used in synchronous detection with a lock-in amplifier. The lock-in amplifier used is a SR850 by Stanford Research Systems. The signal is acquired directly using a homemade LabVIEW software.

Faraday probe setup

Our research goal is to probe the coupling of the surface acoustic waves generated in the substrate by the TG and the average out of plane magnetization component. In order to pursue this result we have combined the TG pump-probe with a magneto-optical analysis of the response to the probe. We integrate our setup with a Faraday spectroscopy configuration, allowing to measure the polarization changes of the transmitted probe beam. The chosen sample is a ferromagnetic Ni thin films of various thickness growth on a glass substrate by electron beam laser deposition. The measurement of the out of plane magnetization change M_z is straightforwardly given by the Faraday rotation.

The Faraday probe setup is the same as the pulsed TG in transmission, except for the final stage sketched in Figure 3. While the pump beams are obtained in the very same way as for the TG setup, the probe consists in the zero diffraction order of the 515 nm beam. As the zero orders of the pump and probe coincide, a color filter is used to get rid of the 1030 nm. This is necessary to avoid additional heat load on sample that could induce some unwanted dynamics.

To study the magneto-elastic coupling, an electromagnet is needed for two main reasons: to set the saturation magnetization of the sample in the wanted direction and to study the dependence of M_z on the applied magnetic field, which should show the expected resonances of the FMR with the SAWs generated by the TG. Figure 1c shows a picture of the sample placed in the air gap. The electromagnet is placed so that it generates an in plane external magnetic field.



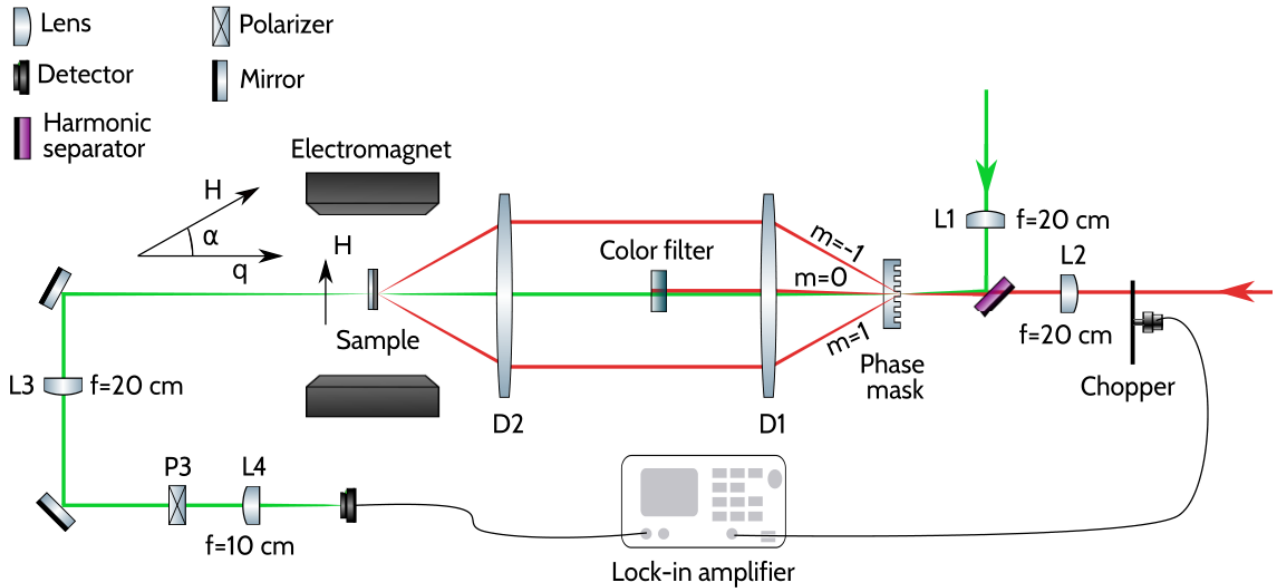


Figure 3: Faraday probe setup. The two first orders of the 1030 nm interfere on the sample generating the TG. The probe consists in the zero order of the 515 nm beam and a filter is needed to separate the two colors. The polarizers P3 is set to reach complete extinction. The electromagnet generates an in plane magnetic.

RESULTS AND DISCUSSION

We performed a systematic study of TG-SAW-driven FMR on polycrystalline Ni thin films of various thickness, that were grown on different substrates, by combining TG excitation and time-resolved (TR) Faraday polarimetry. In this way, we are sensitive to the out-of-plane (OOP) component of the Ni magnetization vector, obtaining information on the coupling between the acoustic and the magnetic degrees of freedom. We also quantitatively estimate the effective magnetization M_{eff} and the Gilbert damping α for the investigated samples. In the case of Ni on CaF_2 substrate, we further compare our SAW-driven FMR results with standard FMR ones on the very same samples, obtaining fully consistent results.

Fig.4 shows the purely acoustic TG signal of Ni (14 nm)/ CaF_2 obtained in transmission geometry with a TG pitch of $\Lambda = 2.5 \mu\text{m}$. A satisfactory fit of the observed intensity (I) oscillations requires two sines, from which we obtain $f_1 = 1.26 \pm 0.06 \text{ GHz}$ and $f_2 = 2.79 \pm 0.02 \text{ GHz}$, corresponding respectively to the Rayleigh Surface Acoustic Wave (RSAW) and the Surface Skimming Longitudinal Wave (SSLW), in agreement with previous studies [7]; the phase velocities ($c = f \Lambda$) are $c_{\text{RSAW}} = 3.2 \pm 0.2 \text{ km/s}$ and $c_{\text{SSLW}} = 7.1 \pm 0.05 \text{ km/s}$.

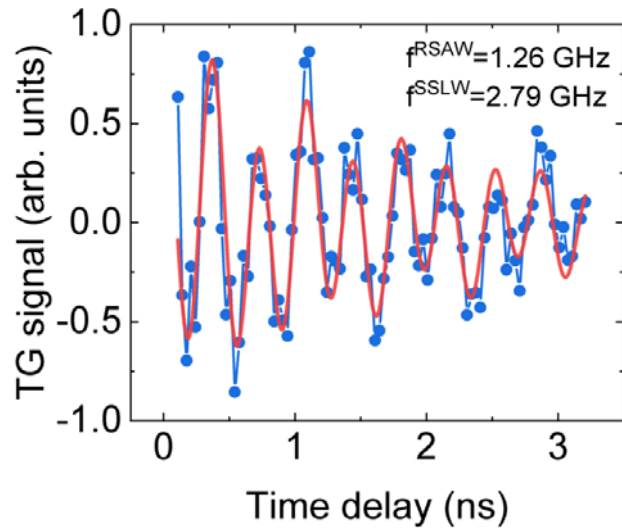


Figure 4: Ni (14 nm)/CaF₂ acoustic TG signal

The magneto acoustic coupling can be extracted by using a probe sensible only to the magnetic part, disentangling the magnetic part (spin wave) to the acoustic part (sound waves), which have to be characterized by the same frequency. By varying the applied magnetic field is moreover possible to separate the two spin waves. In fact, when a ferromagnetic resonance between the applied field and the spin waves is reached, only the corresponding spin wave can be detected.

The results obtained with the Faraday probe are reported in Figure 5.

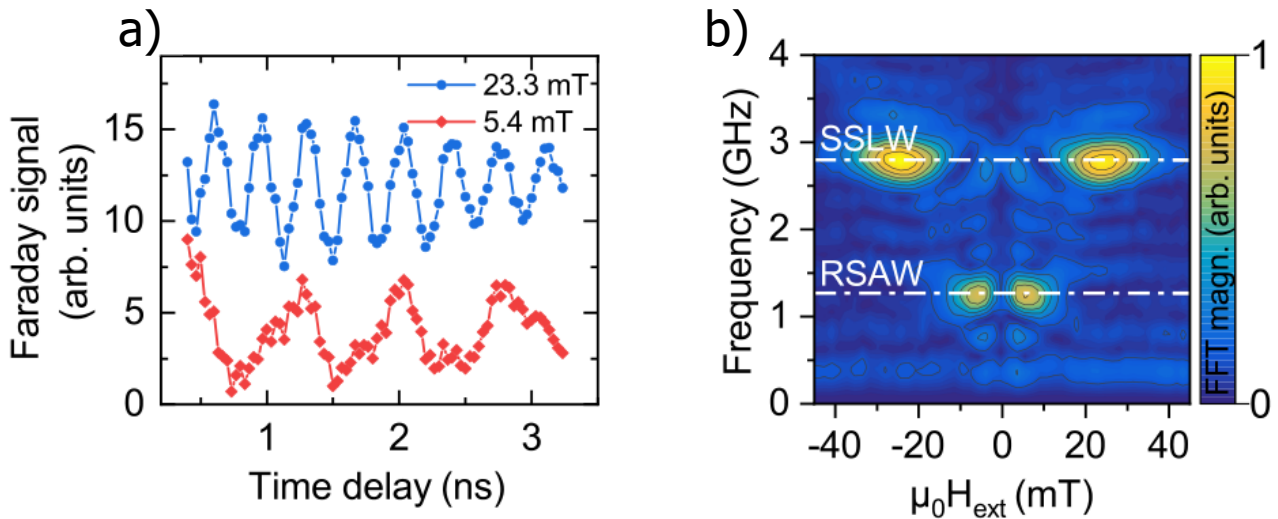


Figure 5: (a) TR-Faraday traces from Ni (14 nm)/CaF₂ at resonance with SSLW (blue dots, $\mu_0 H_{\text{ext}} = 23.3$ mT) and RSA (red diamonds, $\mu_0 H_{\text{ext}} = 5.4$ mT), with $\Lambda = 2.5$ μm . The traces are vertically offset for clarity. (b) 2D FFT magnitude map of each trace in panel (a). The dash-dot red lines at 1.26 and 2.79 GHz correspond to the frequency respectively of the RSAW and SSLW, identifying magneto-elastically-enhanced magnetization precession.

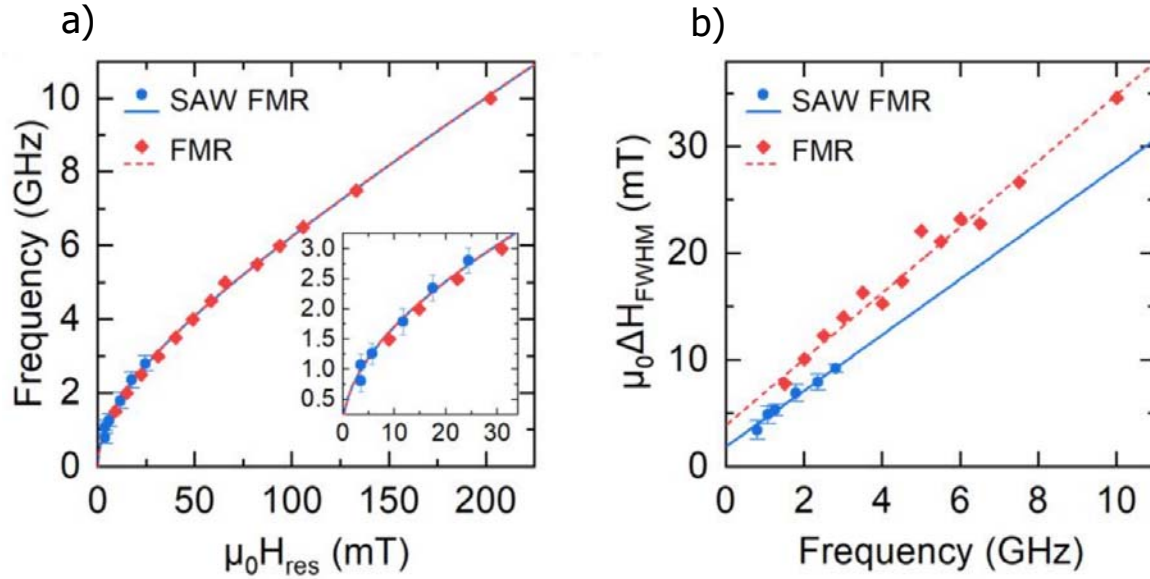


Figure 6: a) SAW-FMR (blue dots) and standard FMR (red diamonds) measurements with the applied magnetic field along the [100] direction. The lines (blue solid for FMR and red dashed for SAW-FMR) are the fits with the Kittel formula (Eq.1). b) Magnetic field FWHM as a function of the resonance frequency. The lines are linear fits (Eq.2). The error bars in the FMR data in panels a) and b) are smaller than the marker size.

We then combine the FFT maps obtained with the three different TG pitches ($\Lambda = 2.5, 3$ and $4 \mu\text{m}$) to extract the SAW-FMR parameters, namely the frequency and magnetic field in resonance condition. Comparison between standard FMR and SAW-FMR is presented in Figure 6. The resonance frequency obtained with both techniques as a function of the magnetic field is reported in panel (a), together with fits of the following Kittel curve:

$$f = \frac{\mu_0 \gamma}{2\pi} \sqrt{H_{\text{eff}}^{\text{res}} (H_{\text{eff}}^{\text{res}} + M_{\text{eff}})} \quad (1)$$

In the fit of standard FMR data, both γ and M_{eff} are free parameters: the best fit is obtained for $\gamma = (2.10 \pm 0.06) \cdot 10^{11} \text{ rad/s}\cdot\text{T}$ and $M_{\text{eff}} = 199 \pm 18 \text{ kA/m}$. Due to the limited SAW-FMR dataset, when fitting it we fixed $\gamma = 2.10 \cdot 10^{11} \text{ rad/s}\cdot\text{T}$; we obtained $M_{\text{eff}} = 195 \pm 16 \text{ kA/m}$, in perfect agreement with what we found from the FMR data.

The linewidth ΔH_{FWHM} of the resonance acquired with FMR and SAW-FMR is reported in Figure 6 (b). For FMR, the linewidth is the FWHM in a sweep of H_{ext} . To compare the FMR and SAW-FMR linewidths, the FWHM value extracted from the SAW-FMR signal along the magnetic field axis of the magnitude of FFT was divided by $\sqrt{3}$: this factor is needed since we work with the magnitude of the FFT rather than with the imaginary part. Following standard analysis from FMR, we extract the Gilbert damping α by fitting the linewidths with the equation

$$\Delta H_{\text{FWHM}} = \frac{4\pi\alpha}{\gamma} f + \Delta H_{\text{inh}} , \quad (2)$$

where ΔH_{inh} is the so-called inhomogeneous broadening term, which is a frequency-independent line broadening due to magneto-structural disorder [43]. For SAW-FMR we obtain

$\alpha = (47 \pm 5) \cdot 10^{-3}$ and $\Delta H_{\text{inh}} = 1.8 \pm 0.5$ mT, again in good agreement with the values obtained from FMR, namely $\alpha = (52 \pm 2) \cdot 10^{-3}$ and $\Delta H_{\text{inh}} = 3.9 \pm 0.4$ mT. We attribute the somewhat larger ΔH_{inh} from FMR to large-scale inhomogeneity that contribute to the FMR signal, as FMR is an area-integrated technique.

In conclusion, we developed a new experimental setup based on FWM approach and a magnetic sensible probe, which allows to generate and detect SAW-FMR. The close comparison of results with standard FMR establishes the validity of SAW-FMR as a method for magnetic and magneto-elastic characterization. The high space resolution of our experimental setup, only limited by the laser focal spot and the SAW wavelength, allows the study of local magnetization dynamic properties of magnetic systems, a condition not achievable using area-integrated techniques (e.g. FMR).

The demonstration to extract spin waves frequencies as a function of induced wave vector, as happening in Brillouin Light Scattering (but in a different wave vector region), allows to access to the DMI constant in an alternative way, directly in the time domain, paying the way to a new approach for magnetic interaction in thin films, extending the applicability also to topological spin structure, where the DMI constant plays a crucial role.

